Global and Planetary Change 137 (2016) 24–34

Contents lists available at ScienceDirect

Global and Planetary Change

journal homepage: www.elsevier.com/locate/gloplacha

Recent temperature trends in the South Central Andes reconstructed from sedimentary chrysophyte stomatocysts in Laguna Escondida (1742 m a.s.l., 38°28 S, Chile)

R. De Jong *, T. Schneider, I. Hernández–Almeida, M. Grosjean

Institute of Geography, University of Bern, Erlachstrasse 9a, 3012 Bern, Switzerland
Oeschger Centre for Climate Change Research, University of Bern, Zähringerstrasse 25, 3012 Bern, Switzerland

ARTICLE INFO

Article history:
Received 7 January 2015
Received in revised form 24 November 2015
Accepted 4 December 2015
Available online 11 December 2015

Keywords:
Anthropogenic warming
Transfer function
Golden algae
Winter temperature
Southern Hemisphere

ABSTRACT

In this study we present a quantitative, high resolution reconstruction of past austral winter length in the Chilean Andes at 38°S from AD 1920 to 2009. For Laguna Escondida, a nearly pristine lake situated on the flanks of the Andes at 1740 m above sea level, past variability in the duration of the winter season (Days $T_{4\,°C}$) was reconstructed. Because high elevation meteorological stations are absent in this region, the reconstruction provides novel insights into recent temperature trends in the central–southern Andes. As a cold-season temperature proxy, we used chrysophyte stomatocysts. This novel proxy for cold season temperature was so far applied successfully in the European Alps and Pyrenees but has not yet been tested in the Southern Hemisphere. The reconstruction in this study was based on a newly developed Transfer Function to estimate Days $T_{4\,°C}$ (number of consecutive days with surface water temperatures at or below 4 °C) from sedimentary stomatocyst assemblages ($R^2_{boot} = 0.8$, $RMSEP_{boot} = 28.7$ days (= half the standard deviation)). To develop a high quality TF model, sediment traps and thermistors were placed in thirty remote lakes along an altitude gradient (420–2040 m a.s.l.). Complete materials and data were collected in 24 lakes after one year. Detailed statistical analyses indicate that modern stomatocysts primarily respond to the length of the cold season. The TF model was then applied to the sedimentary stomatocysts from a ^{210}Pb-dated short core of L. Escondida. Comparison to independent reanalysis data showed that reconstructed changes in Days $T_{4°C}$ provides detailed information on winter–spring temperature variability since AD 1920.

The reconstruction shows that recent warming (onset in AD 1980) in the southern Chilean Andes was not exceptional in the context of the past century. This is in strong contrast to studies from the Northern Hemisphere. The finding is also in contrast to the cooling temperature trends which were detected using meteorological measurement data in low altitude sites along the Chilean coast. This finding confirms that coastal meteorological station data in this region do not reliably reflect recent temperature trends at high altitudes. Moreover, it implies a southward shift of the northern border of the Westerlies wind belt. This study clearly illustrates the importance of quantitative, high resolution studies from remote sites, in particular at high elevation mountain areas.

© 2015 Elsevier B.V. All rights reserved.

1. Introduction

Anthropogenic warming is one of the most important and most debated topics of our time. To place the extent and rate of anthropogenic warming in a long-term perspective, long term reconstructions are required. For the Northern Hemisphere a large number of temperature measurements and reconstructions are available at high resolution and high quality and going back far in time. For the Southern Hemisphere, the number of high-resolution, quantitative temperature reconstructions are substantially smaller, not only for Africa but also for South America (e.g. PAGES 2 k Consortium, 2013). For large parts of South America, meteorological data are unavailable or incomplete, whereas high-resolution, quantitative proxy-based reconstructions are scarce (e.g. Neukom et al., 2010a,b). Although Chile is comparatively well-studied in the South American context, meteorological time series in southern and central Chile are sparse in a spatial as well as a temporal sense. Meteorological measurement data are rarely available prior to AD 1950 and most meteorological time series that do extend to AD 1950 are incomplete. In addition, the majority of meteorological stations in the southern and central part of Chile are located at low elevations (Falvey and Garreaud, 2009). Hence, very little is known about recent temperature variability in the Andes. Interestingly, Falvey and Garreaud (2009) showed that coastal meteorological stations in central–southern Chile display delayed warming or even cooling since ca AD 1970. It is currently not known whether mountain areas in central

* Corresponding author.
E-mail address: dejong@giub.unibe.ch (R. De Jong).

http://dx.doi.org/10.1016/j.gloplacha.2015.12.006
0921-8181/© 2015 Elsevier B.V. All rights reserved.

and southern Chile also experienced cooling in recent decades. In summary, without additional data from high altitudes in this region, it is not possible to place temperature trends measured at low elevation station data for the past few decades in a wider spatial and temporal context. Therefore high-resolution reconstructions of past climate variability are much needed, in particular from higher altitudes.

In this paper we present a high-resolution climatic reconstruction from Laguna Escondida situated along the Andean ridge at 38°28′S (Fig. 1) at an elevation of 1742 m above sea level. The reconstruction covers the period AD 1920 to 2010. This reconstruction is based on a newly developed Transfer Function that uses chrysophyte stomatocysts as a proxy for the length of the winter season. Chrysophytes (*Chrysophycae*, *Synurophyceae*; the golden algae) produce siliceous stomatocysts that are usually well-preserved in lake sediments. Previous work on stomatocysts in the Alps and Pyrenees has shown that stomatocyst composition in mountain lakes is predominantly controlled by winter–spring temperatures (Kamenik and Schmidt, 2005; Pla and Catalan, 2005; De Jong and Kamenik, 2011). De Jong and Kamenik (2011) hypothesized that the influence of winter–spring temperatures was through its control on the timing of lake ice break up and hence the total duration of ice cover on a lake. Other studies, however, demonstrate the importance of lake water conductivity and ion composition on stomatocyst assemblages (Duff et al., 1995; Zeeb and Smol, 1995, Pla et al., 2003; Pla and Anderson, 2005; Hernández-Almeida et al., 2014). Here we explore the use of stomatocysts as a proxy for winter–spring environmental conditions in the Chilean southern Andes. We used the 'number of consecutive days with surface water temperatures at or below 4 °C' ($DaysT_{4\ °C}$) as a proxy for the length of the ice-covered (or cold) season for high (low) altitude lakes. To our knowledge, this is the first time that stomatocysts are used as a quantitative climatic proxy in South America.

Because quantitative reconstructions using Transfer Functions are much debated in recent literature, we then discuss the selection criteria used to find the most important environmental parameters, the strengths and weaknesses of the TF-model and the potential influence of co-varying variables other than temperature (Telford and Birks, 2011; Juggins, 2013). Laguna Escondida was selected for the reconstruction based on the characteristics of the training set data. The reconstruction for the period AD 1920–2009 allows for a comparison with independent reanalysis data and meteorological data from low elevation sites. This reconstruction provides important insights into high altitude temperature variability and recent trends since AD 1920. Moreover, it provides data on climatic variability during the cold season, which is highly unusual since most natural proxies are biased towards the warm (growing) season (Jones et al., 2009).

2. Study area

In this section we first describe the climatic set-up and main geological features of the study area for which the training set was developed. Next, we describe the morphological and biological characteristics of the catchment area of L. Escondida (38°28′37 S; 70°58′54 W).

2.1. Training set

2.1.1. Climatic set-up

The study area is situated in the eastern part of the 9th and 10th administrative districts in Chile (Región de Bío-Bío and Región de Araucanía). It covers the Chilean side of the Andes just north of Patagonia (36–39°S). In winter this region is primarily influenced by the strength and position of the southern Hemisphere Westerlies. Analyses of large-scale weather patterns by Garreaud et al. (2009, 2013) show that in the study area, there is strong covariability between low-level zonal air flow and precipitation. This is particularly pronounced on the western flanks of the Andes due to orographic effects (Garreaud et al., 2013). The influence of westerly flow on temperature in the study area differs per season. Winters (JJA) with strong (weak) westerly flow are characterized by mild (cold) air temperatures in the study area (Garreaud et al., 2013). Temperatures during the other seasons are also influenced by other factors, such as sea surface temperatures and temperatures aloft.

There are no meteorological stations at high elevations in or near the study area. To describe regional climate parameters we use data from the nearest meteorological station (Temuco, Fig. 1), which is situated in the Central Valley of Chile (at ca. 126 m a.s.l., 140 km west of L. Escondida). Winters in Temuco are relatively mild and wet (mean JJA temperature 1980–2010: 7.3 °C, mean JJA precipitation: 162 mm), whereas summers are warm and dry (mean DJF temperature 1980–2010: 15.5 °C, mean DJF precipitation: 39 mm). Annual precipitation amounts to 1150 mm (average of total annual precipitation AD 1980–2010). For comparison to the reconstruction presented in this paper, reanalysis data for temperature from the 0.5° × 0.5° grid cell encompassing Laguna Escondida were used (Mitchell and Jones, 2005). Precipitation data were not used because of the sparsity of data and the long distance to the nearest meteorological station, and the strong orographic effects that influence precipitation in mountain regions.

2.1.2. Geology

The study area is characterized by the Andean ridge and the presence of a large number of active and dormant volcanoes. Both features are the result of the ongoing subduction of the oceanic Nazca Plate under the South American Plate (Parada et al., 2007). In the northern part of the study area, the highest elevations (up to 3000 m) are found along the main Andean ridge. The southern part of the study area lies on the western flanks of the Andean ridge (altitudes up to ca 1500 m). The entire area, but in particular the southern half, is characterized by volcanoes reaching up to 3775 m (Volcán Lanín). On average, the volcanic chain of Chile (from 33 to 46°S) has experienced one volcanic eruption each year in postglacial times (Parada et al., 2007). The bedrock in the study area is composed of recent and old volcanic products as well as igneous bedrocks, and is dominated by basaltic lava and pyroclastic materials (tufas, breccias) (Parada et al., 2007).

2.1.3. Training set lakes

The lakes in the training set were chosen along an altitude gradient (420–2040 m a.s.l.) with the aim of covering a long temperature gradient. The lakes in the training set are diverse, however, their geological settings are highly comparable because the entire region along the Andean ridge is dominated by igneous as well volcanic bedrock types and calcareous ones are absent (Servicio Nacional de Geologia y Mineria, 2003). A clearly visible gradient along altitude was the density, type and presence of vegetation, and similarly the thickness and presence of soils. Around the highest lakes in the training set, soil was present only as thin, spread out patches and vegetation was limited to low grasses and mosses. At the mid and low altitude lakes vegetation ranged from dense forests to agricultural land on well-developed soils.

An important indirect temperature gradient in the dataset is the level of freezing. All lakes situated above 1200 m a.s.l. (16) were frozen during the winter of 2011, whereas below that altitude only one lake had ice cover during winter. The consecutive number of days with surface water temperatures at or below 4 °C, or $DaysT_{4\ °C}$, ranged from 0 to 216 days (Table 1). An additional important environmental gradient is land use. Whereas land use was very extensive or absent in all lakes above 1100 m, several lakes at lower altitudes were situated in or nearby agricultural land (in particular L. Menetue, L. San Jorge, L. Icalma and L. Icalma-chica). The presence or absence of land use influences the chemical composition of the lake water, which affects ion compositions as well as conductivity values.

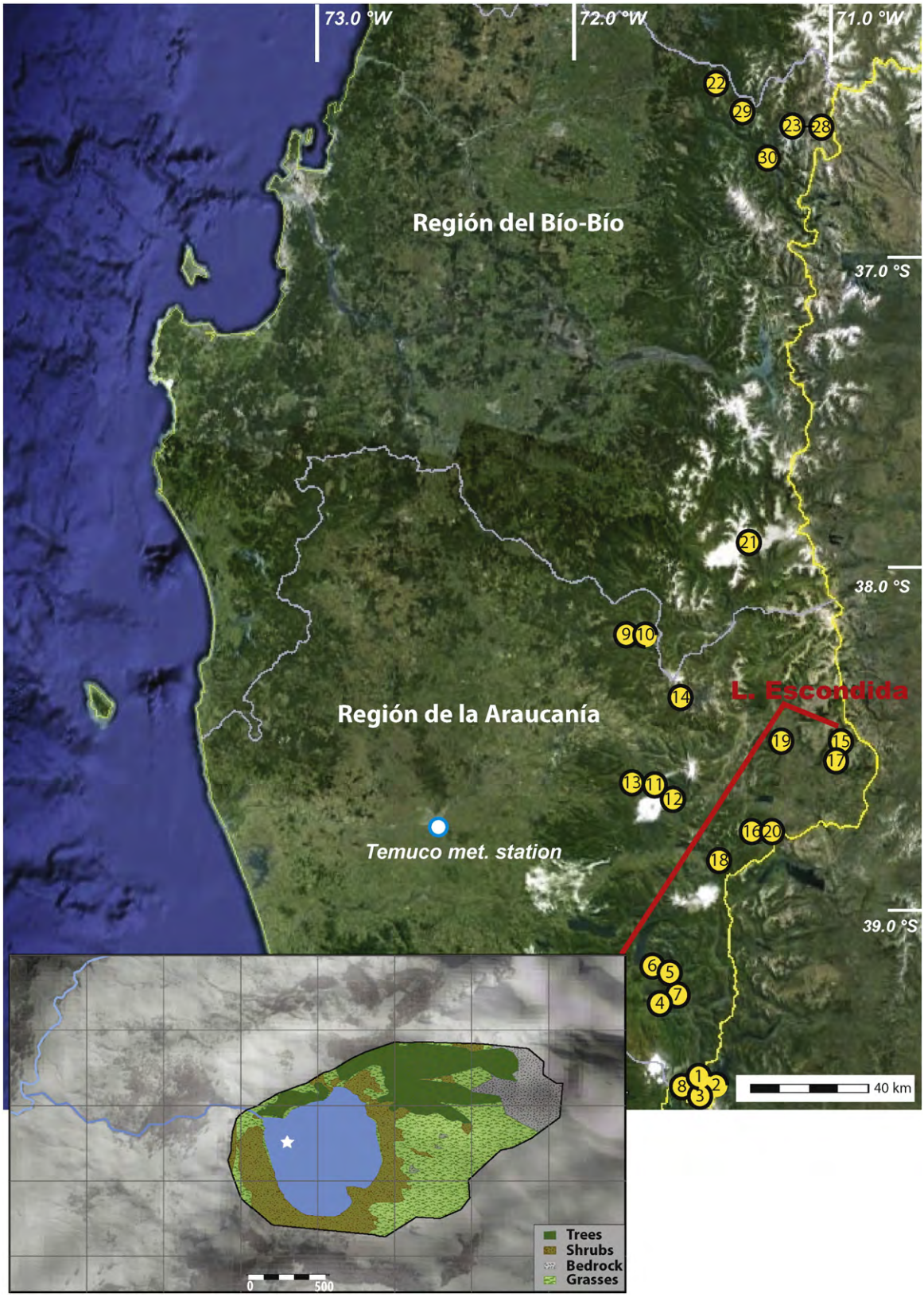

Fig. 1. Overview map of the study area, showing the location of all thirty lakes (see below) which were equipped with sediment traps and thermistors. Lake names in italics were not included in the final analyses because sediment traps and thermistors could not be recovered after one year of exposure. The inset shows Laguna Escondida and its catchment and vegetation characteristics. The coring location is indicated with an asterisk. The position of the nearest meteorological station, Temuco, is also shown. 1) L. Quilluehue, 2) *L. Huinfiuca*, 3) L. Verde, 4) L. Menetue, 5) L. Llancalil, 6) *L. Tinquilco*, 7) L. San Jorge 8) L. Escondida, 9) *L. Malleco*, 10) L. Verde, 11) L. Captrén, 12) *L. Verde*, 13) *L. Negra*, 14) *L. Blanca*, 15) L. Escondida (reconstruction in this study), 16) L. Icalma-chica, 17) L. Verde, 18) L. Sta Olga, 19) L. San Pedro, 20) *L. Icalma*, 21) L. La Mula, 22) L. Verde, 23–25) Tres Lagunas I, II and III, 26) El Baúl (top), 27) El Baúl (mid), 28) L. Fuentecillas, 29) L. La Plata, 30) L. Chacayal.

Table 1
Summary statistics of 29 environmental variables measured in 23 lakes in the study area (Lake Menetue was excluded). Variables in italics were included in subsequent analyses.

	Unit	Minimum	Maximum	Mean	Median	St dev
Lake parameters						
Relative lake depth	m	$3.1 \cdot 10^3$	$107.3 \cdot 10^3$	$20.9 \cdot 10^3$	$9.3 \cdot 10^3$	$27.5 \cdot 10^3$
Lake area	ha	2	196	26	13	45
Lake depth	m	2.7	57	13.8	11.9	10.8
Secchi depth	m	2.3	16.4	7.9	7	4.1
Temperature variables						
Days $T_{4\,°C}$	# days	0	216	138.6	163	60.2
DJF temp	°C	11.2	22.3	16.9	16.7	2.7
MAM temp	°C	6.5	14.6	10.9	10.9	1.8
JJA temp	°C	4	6.9	4.4	4	0.7
SON temp	°C	4	13.9	6.5	5.5	3.1
JJASON temp	°C	4	10.2	5.4	4.7	1.8
DJFMAM temp	°C	10.6	18.4	13.9	13.5	2.1
Annual mean temp	°C	5.2	12.8	7.7	6.9	2.2
Lake water chemistry						
Conductivity	$\mu S\ cm^{-1}$	43.5	174.8	69.7	54.7	32.3
Dissolved O_2%	%	77.6	130.1	93.4	92.6	14.1
pH		6.3	8.5	7.1	7.1	0.5
Na	$mg \cdot L^{-1}$	0.4	7.2	2.0	1.6	1.8
K	$mg \cdot L^{-1}$	0.1	2.0	0.5	0.4	0.4
Mg	$mg \cdot L^{-1}$	0.07	4.29	1.05	0.58	1.17
Ca	$mg \cdot L^{-1}$	0.76	11.01	3.33	2.07	2.78
Fe	$mg \cdot L^{-1}$	0	0.03	0.01	0.009	0.007
Al	$mg \cdot L^{-1}$	0	0.017	0.006	0.006	0.005
Cl	$mg \cdot L^{-1}$	0.16	1.09	0.57	0.50	0.32
Si	$mg \cdot L^{-1}$	0.28	11.33	4.10	2.71	3.23
SO_4	$mg \cdot L^{-1}$	0.15	7.66	1.30	0.77	1.66
Lake water nutrients						
Total N	$mg \cdot L^{-1}$	0	0.44	0.07	0.04	0.11
P in PO_4	$\mu g \cdot L^{-1}$	0	12.06	1.78	0.91	3.05
N in NO_2	$\mu g \cdot L^{-1}$	0	0.27	0.05	0	0.08
N in $NO_2 + NO_3$	$\mu g \cdot L^{-1}$	0	8.91	1.80	0.77	2.51
N in NH_4	$\mu g \cdot L^{-1}$	1.93	62.64	9.16	6.37	11.99
Lake water carbon content						
DOC	$mg \cdot L^{-1}$	0.09	4.02	1.69	1.53	0.96
DIC	$mg \cdot L^{-1}$	0	13.88	3.96	2.78	3.56

2.2. Laguna Escondida

L. Escondida (No. 15 in Fig. 1) lies in the natural reserve of Alto Bío-Bío, at the edge of a plateau above the Pehuenco River Valley. The lake is situated at 1742 m, has a maximum depth of 17.8 m and covers ca. 30 ha. It has a small catchment of 1.5 km^2 and does not have permanent inflows. A small, non-permanent outflow into the Pehuenco River Valley is situated at the northwestern edge of the lake. The catchment is characterized by bare bedrock of volcanic origin in the steep upper parts and grassland on the gentler slopes, whereas the lake itself is surrounded by, in part, dense vegetation of *Nothofagus* trees and bushes (*Nothofagus pumilio* and *Nothofagus antarctica*) and *Araucaria* trees (*Araucaria araucana*). A small wetland with mosses is present at the northeastern edge of the lake. Land use is very extensive. The presence of a small animal shed just outside the catchment area indicates that it is likely that a small number of goats or horses use the area for grazing at times.

Lake surface water conductivity (68 μS/cm), pH (7.1) and oxygen saturation (83%) were measured on three occasions, all in summer. During these measurements the lake was weakly stratified to unstratified. Lake water transparency was assessed using a Secchi-disk, giving a Secchi depth of 14.5 m. Combined with low orthophosphate (1.5 μg/L) and total nitrogen (0.06 mg/L) contents, this indicates that the lake is oligotrophic. Thermistor measurements show that during the winter of 2011 ice cover lasted for 134 days, from the 5th of June to 17th of October. Thermistor data also suggest that the lake is dimictic.

3. Methods

Here we first describe the methods required for the development of the chrysophyte stomatocyst environmental training set: training set design, collection of environmental data, stomatocyst analysis and numerical analyses. In the second part we describe methods used to provide an environmental reconstruction back in time based on the sediment core from L. Escondida: sediment analyses, dating and numerical methods.

3.1. Field work strategy and laboratory methods

Chrysophyte stomatocysts are known to be sensitive indicators of, among other parameters, the duration of lake ice cover and hence cold-season temperatures (Kamenik and Schmidt, 2005; Pla and Catalan, 2005, De Jong and Kamenik, 2011). The training set in this study was therefore designed to maximize the temperature gradient. Thirty lakes were selected along an altitudinal gradient ranging from 420 to 2040 m a.s.l. At the same time, the latitudinal extent of the training set was kept small (from 36.3 to 39.3°S) to minimize differences in insolation. Each lake was equipped with a sediment trap placed with the tube opening ca 1.5 m above the sediment surface and a thermistor at ca. 1 m below the water surface (Bloesch and Burns, 1980). Traps were placed in the deepest part of each lake, which was located using a handheld echo sounder. Traps and thermistors were left for the duration of one year (from Jan. 2011 to Jan. 2012), after which the accumulated sediments were collected and data read out. Using this approach, the sediment composition could be linked directly to measured water temperatures. After one year of exposure, 24 out of 30 traps were recovered.

For each lake 47 environmental parameters were assessed (partly listed in Table 1). These parameters describe lake water composition and chemistry, and catchment characteristics such as vegetation type and density, land use and bedrock types. Lake water conductivity, oxygen saturation, pH and temperature were measured along lake depth using a multiparameter system YSI 600QS. Data shown in Table 1 represent the average values for the epilimnion. Lake water transparency was assessed using a Secchi disk. Ion composition was determined for samples from the epi-, meta- and hypolimnion, using ion chromatography (chloride, sulfate), ICP-OES (Na, K, Mg, Ca, Fe and Al) and spectrophotometry (S). Lake water nutrients (forms of N and P) were measured using a Skalar auto-analyzer (Koroleff, 1976; Grasshoff, 1976). Total nitrogen was measured using a flow injection analyzer. Dissolved organic and inorganic carbon was determined with a TOC-5050A Shimadzu. All temperature measurements were derived from thermistor data (Vemco Minilog II) which measured surface water temperature every 30 min for the duration of one year.

After one year, sediment traps and loggers were carefully lifted into the boat and water was siphoned off the traps. The remaining 1 L of sample (2 holders of 500 mL for each lake) was oven dried at low temperatures (50 °C). Sediments were subsequently scraped and rinsed out, freeze-dried and prepared for stomatocyst analyses. Treatment of these samples was identical for each lake and consisted of treatment with H_2O_2 (up to 5 days, waterbath at 80 °C, to remove organic carbon) and washing with deionized water. Next, a subsample of the sediment solution was allowed to settle overnight onto a scanning electron microscope graphite planchet. All stomatocyst analyses were carried out using a scanning electron microscope (ZEISS-EVO40). For each lake a minimum of 400 stomatocysts was photographed and classified according to size, collar and/or pore morphology and outer wall ornamentation. Because this is the first large scale, detailed analysis of stomatocysts in this region, no reference work was available for classification.

3.2. Training set, numerical methods

3.2.1. Correlation between stomatocyst assemblages and environmental variables

DCA (detrended correspondence analysis) was carried out to determine the gradient length of the stomatocyst dataset, resulting in a gradient length of 2.5 standard deviations (SD). Hence, unimodal response models were required for further analyses (Ter Braak, 1987). Percentages were calculated and stomatocysts were square-root transformed to stabilize their variance. Only stomatocysts with an abundance >2.5% and an occurrence in at least two lakes were retained for further analyses. A large number of environmental variables displayed a non-normal distribution. These variables (relative depth, conductivity, total N, K and DOC) were log- transformed. All analyses were carried out in R (R development core team) using the packages Vegan (Oksanen et al., 2013), packfor (Dray et al., 2013) and hier.part (Walsh and Mac Nally, 2013).

Because the total number of measured environmental variables (47) exceeded the number of observations, a reduction of variables was required prior to further analyses. Therefore, all highly correlated ($R > 0.8$) variables were reduced, retaining those that described environmental variability best (e.g. conductivity was retained, whereas Na, Mg, Ca, Cl and DIC were removed). Thermistor-based temperature data could not be used directly. Because 16 out of 23 lakes froze over during the winter season, surface water temperature measurements for these lakes were truncated at 4 °C. At 4 °C, water reaches its highest density and can start to freeze. Temperatures below 4 °C were also measured when thermistors were frozen into the ice. However, these temperature values are not reliable because they primarily depend on the depth of the thermistor in relation to the water surface. In lakes where natural surface level fluctuations occur, values below 4 °C thus reflect the thickness of the ice in relation to absolute thermistor depth at the time of freezing, which is not a variable of interest.

We therefore derived an index for the total number of consecutive days with surface water temperatures at or below 4 °C ($DaysT_{4\ °C}$). This index captures the variability in winter length among all lakes. Lakes with ice cover were distinguished from lakes without ice cover by comparing the daily temperature variability during the winter months (near-constant temperatures at or below 4 °C indicate ice cover) in detail. Because $DaysT_{4\ °C}$ was highly correlated with surface water temperatures during winter and spring (JJASON, $R = -0.98$), these months were removed from the analyses. After these initial steps, 18 environmental variables were left (Table 1). The correlations between these variables are shown in Supplementary Material 1.

CCA (canonical correspondence analysis) was carried out to assess the influence of environmental variables on stomatocyst compositions and to identify unusual stomatocyst assemblages or values of environmental variables (Ter Braak, 1987). Next, a number of approaches were used to find the environmental variable that explained most of the variance in the stomatocyst dataset. 'Classic' forward selection was used to find the most important environmental variables, however, by default this method excludes variables that are strongly correlated (Juggins, 2013). Elevation was therefore removed prior to further analyses. The more strict forward selection approach suggested by Blanchet et al. (2008) was also applied. This approach uses the alpha significance level as well as the adjusted coefficient of multiple determination (R^2_a) calculated using all explanatory variables. VIF's (variance inflation factors) were calculated to detect variables (VIF > 20) with a strong multi-collinearity (Ter Braak, 1988). Since these approaches yielded different results, marginal effects and their significance were calculated for all remaining variables by determining the partial CCA (Kamenik and Schmidt, 2005). Marginal effects provide the percentage of variance in the stomatocyst dataset that is explained individually by an environmental variable (higher is better). Hierarchical partitioning (Juggins, 2013) was then used to assess the shared and individual explained variance for the environmental variable of interest. Finally, the ratio of the first constrained CCA eigenvalue to the first unconstrained eigenvalue ($\lambda1/\lambda2$) was calculated (Juggins, 2013). This ratio determines the ability of the variable to maximize the dispersion of the scores for each stomatocyst type. Ideally, $\lambda1/\lambda2$ exceeds 1, indicating that the variable of interest explains more variance in the dataset than an unknown, underlying variable (or set of variables) represented by the first CA axis.

3.2.2. Transfer function development

The following models were tested to establish a Transfer Function: Weighted Averaging using unweighted classic and inverse deshrinking (WAclass and WAinv), Weighted Averaging–Partial Least Squares (WA-PLS), Maximum Likelihood (ML) and a Modern Analog Technique (MAT), as implemented in the computer program C2 (Juggins, 2003).

The minimal adequate model ideally has a combination of a high coefficient of determination (R^2) between observed and predicted values, low mean and maximum bias and a low root mean squared error of prediction (RMSEP). All these values were assessed by cross-validation (bootstrapping, 999 permutations; Birks, 1995). In WA and WA-PLS, only components leading to a significant reduction in RMSEP (5% or more) were retained (Birks, 1995). The minimal adequate model was examined for potential outliers, because these can strongly affect Transfer Function coefficients.

3.3. Analyses of sediment core Laguna Escondida

In January 2011 a 48 cm long sediment core was collected from the deepest basin (17.8 m) in L. Escondida (Fig. 1). In the laboratory, the core was split lengthwise in two halves (Esc.A and Esc.B). Both core halves were photographed, sediment structures were described in detail and scanning methods (VIS-RS scanning, Magnetic Susceptibility; Trachsel et al., 2010) were applied. Esc.A was subsampled in 2 mm samples throughout the core, whereas Esc.B was used primarily for dating purposes. All subsamples were freeze-dried and the water content was determined by calculating weight loss after drying.

The top 10 cm of core half Esc.B was subsampled in 5 mm samples. From this section, 15 samples were selected for ^{210}Pb dating using α-decay counts. In addition ^{226}Ra was measured on three samples to establish the level of supported ^{210}Pb (Appleby, 2001), and ^{137}Cs was measured to serve as an additional (independent) chrono-marker. Both the CIC (constant initial concentration) and CRS (constant rate of supply) models were tested to establish the most suitable age-depth model (Appleby, 2001; Von Gunten et al., 2009).

Stomatocyst analysis was carried out on all 2 mm samples in the top 10 cm of Esc.A (50 samples). For each sample a minimum of 50 specimens was counted (average 83 specimens). To provide a sufficiently high total sum of specimens for the reconstruction, we used running sums of 3 consecutive samples (yielding an average total sum for each datapoint of 240 specimens, minimum: 158, maximum: 787). This approach gives a total count which is sufficiently high to interpret changes in rare taxa, whereas the fine subsampling allowed us to pinpoint rapid changes in abundant taxa at a high resolution. The minimal adequate model was applied to the down core stomatocyst data. Squared chord distances were calculated to assess similarities between the fossil and modern stomatocyst assemblages.

4. Results

4.1. Training set data

In Table 1 the mean values, standard deviations and other characteristic values of 31 measured environmental variables are summarized. These values reflect conditions in the 24 lakes for which all data and materials were recovered after one year of trap-exposure, excluding the data for Lake Menetue (outlier). Stomatocysts were analyzed for the same lakes. This resulted in the classification of >120 different

stomatocyst types whereas the total number of stomatocyst types greatly exceeded this number (stomatocyst types were classified only if more than five specimens could be clearly identified). Seventy-two stomatocyst types were used for subsequent analyses because the abundance exceeded 2.5% and they occurred in more than one lake. The ten most common species in the training set are depicted in Supp. Mat. 2. Their relation to published stomatocyst types is shown in Supp. Mat. 4.

4.2. Relations between environmental data and modern stomatocyst assemblages

A CCA on all 18 environmental variables showed that Lake Menetue contained stomatocyst types that were significantly different from all other lakes. This lake was also an outlier in terms of environmental parameters; it was located at a very low altitude (370 m) and annual temperatures were the highest (12.83 °C). It was therefore removed prior to subsequent analyses. In addition, two outlier stomatocyst types were identified and removed. The PCA biplot for the remaining lakes (Fig. 2) illustrates the relations between variables. The first PCA axis explains 32% of the variability in the dataset and is primarily driven by temperature variables ($DaysT_{4\,°C}$, DJFMAM) as well as conductivity and Si. The PCA biplot further illustrates the high (anti)correlations of conductivity, Si, $DaysT_{4\,°C}$ and DJFMAM with elevation. These relations are further discussed in Section 5.1 and Fig. 5.

The CCA biplot for the same lakes (Fig. 2) shows a comparable pattern, with conductivity and $DaysT_{4\,°C}$ as the most prominent variables along the first axis. Elevation and summer temperatures (DJFMAM) are also important along the first axis. Along the second axis, variability in nutrient content (Total N and N in $NO_2 + NO_3$, DOC, phosphorus) appears dominant. The high influence of Total N, however, is driven by a single lake (L. San Pedro) and its importance should therefore not be overestimated.

Classic forward selection on the environmental parameters indicated that Si and K are important environmental variables determining stomatocyst assemblages in the training set data, followed by $DaysT_{4\,°C}$. Forward selection using the (stricter) R^2_a criterion however, resulted in significant results for '$DaysT_{4\,°C}$' only. VIF's were >20 for the variables 'P in PO_4' and 'DJFMAM temperature'. These variables were removed because a value above 20 indicates multi-collinearity. Marginal effects and their significance were then calculated for all variables (Table 2). Variables that are not listed in Table 2 did not explain a significant part of the variability in the stomatocyst dataset in a partial CCA. Variables were ordered along their $\lambda1/\lambda2$ scores.

Table 2 shows that 'Si', '$DaysT_{4\,°C}$' and 'Conductivity' have the highest $\lambda1/\lambda2$ scores. None of the variables yielded a $\lambda1/\lambda2 > 1$. Since none of the statistical indicators in Table 2 is conclusive as to which variable summarizes variance in the stomatocyst dataset best, we developed a Transfer Function for each of the three variables with an overall high 'score' in Table 2.

Table 2
Environmental variables with significant ($p < 0.05$) marginal effects (i.e. percentage of variance they explain individually). The ratio of the first constrained (CCA1) eigenvalue to the first unconstrained (CA1) eigenvalue ($\lambda1/\lambda2$) determines the strength of the variable in its ability to maximize the dispersion of the taxon scores. The variables are ordered according to this measure.

	Marginal effect	$\lambda1/\lambda2$	Sign. of partial CCA (p-value)
Si	0.11	0.83	<0.01
Days $T_{4\,°C}$	0.11	0.83	<0.01
Conductivity	0.10	0.83	<0.01
K	0.10	0.79	0.01
Diss. O_2%	0.09	0.67	0.001
Total N	0.05	0.35	not sign.

4.3. The minimal adequate model

Table 3 shows the main criteria used to assess model performance using '$DaysT_{4\,°C}$' as the explanatory variable of variability in the stomatocyst dataset. The same calculations were made for 'Si' and 'Conductivity', however, these yielded a very low R^2_{boot} of 0.3. The table shows that the bootstrapped WA-PLS2 model for '$DaysT_{4\,°C}$' has a high predictive power ($R^2_{boot} = 0.8$), the smallest model error and comparatively small values for maximum and mean bootstrapped bias. The choice for the more complex WA-PLS2 model is justified since the improvement of the RMSEP in comparison to the simpler WA-PLS model exceeds 5% (Birks, 1995). The $RMSEP_{boot}$ of 28.7 $DaysT_{4\,°C}$ is roughly half of the standard deviation of $DaysT_{4\,°C}$ measured in the training set lakes (Table 1).

Fig. 3 illustrates the Transfer Function model performance and residual structure. The observed and predicted '$DaysT_{4\,°C}$' are in good general agreement (hence the high R^2). The residuals display a trend. Winter temperature values (JJASON) values are truncated at 4° but otherwise strongly correlated with $DaysT_{4\,°C}$. $DaysT_{4\,°C}$ was not truncated and was therefore used instead of the direct water temperature measurements.

4.4. Laguna Escondida age-depth model

In Fig. 4a the results for the total activity of ^{210}Pb and ^{226}Ra and the flux values for ^{137}Cs measurements are plotted along sediment depth.

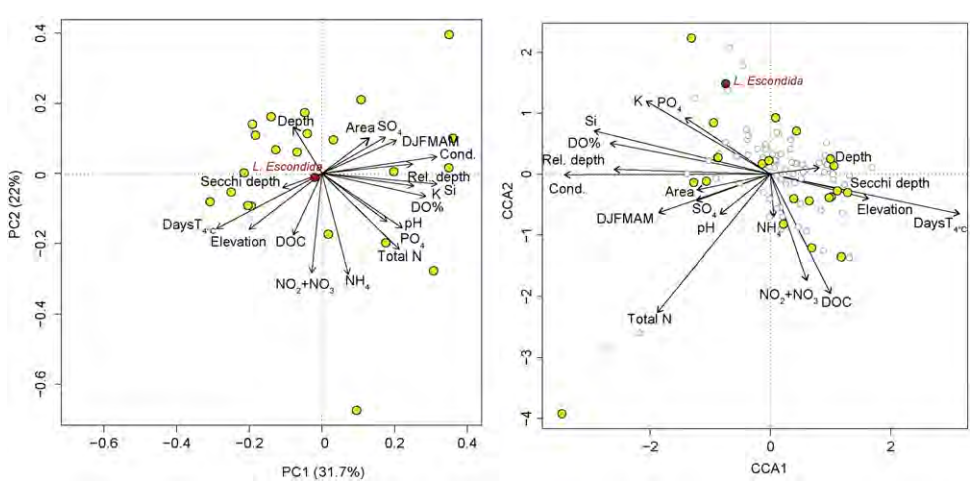

Fig. 2. PCA and CCA biplots showing the relative importance of environmental variables along the first and second axes. Variables as shown in Table 1.Yellow dots mark lakes in the training set, white dots show species scores.

Table 3
Descriptive statistics for a number of 'Days $T_{4\,°C}$ inference models. Three stomatocyst types and one lake (Lake Menetue) were not included in these model runs. The weighted averaging–partial least square model with 2 components (WA-PLS2) is the best performing model, with the highest R^2_{boot}, smallest $RMSEP_{boot}$ and smallest bias. The significant 9.7% improvement of the WA-PLS2 with respect to the WA-PLS1 model justifies the choice of the more complex WA-PLS2 model (Birks, 1995).

	WA-inv	WA-class	WA-PLS1	WA-PLS2	ML	MAT
R^2_{boot}	0.75	0.76	0.75	0.80	0.63	0.67
$RMSEP_{boot}$	32.1	30.7	31.85	28.74	48.47	44.4
Max $bias_{boot}$	70	62	70	49	122	109
Mean $bias_{boot}$	0.22	0.23	−1.2	−0.48	−11.5	−12.6
% change		4.2		9.7*		

The ^{210}Pb profile follows an overall pattern of exponential decay from a relatively low initial total activity of 200 Bq kg^{-1} (of which 10 Bq kg^{-1} are supported) down to 22 cm sediment depth. At that depth, the ^{210}Pb profile reaches the supported activity level as indicated by the ^{226}Ra measurements. The ^{137}Cs curve increases sharply around 6.8 cm depth, which we associated with the beginning of detectable ^{137}Cs fallout in most parts of the world between AD 1952 and 1954 (Basran, 2011). This level was used to constrain the CRS model. The 'classic' ^{137}Cs peak value (AD 1964) and decrease towards modern time were not detected in the core from L. Escondida.

Fig. 4b shows the age-depth model based on the CRS model, the constrained CRS model and the CIC model. The CIC model shows multiple age-reversals and was therefore not selected. The unconstrained CRS model assigns the first increase of ^{137}Cs (ca. 6.8 cm) and subsequent high ^{137}CS values to ca AD 1965 and later, which is clearly incorrect since values are known to decrease after AD 1964. We therefore selected the constrained CRS model as the most suitable one.

For the time period AD 1950–present, the constrained CRS age-depth model has small dating uncertainties of five years maximum. Prior to AD 1950 the dating uncertainty increases up to ±10 years around AD 1930.

4.5. Laguna Escondida: stomatocyst-based reconstruction of 'Days$T_{4\,°C}$'

The variability over time in the 27 most common stomatocyst types are shown in Fig. 5. Squared chord distances, reflecting the analogy between stomatocyst assemblages in the training set and the sedimentary stomatocyst assemblages, generally exceeded the tenth percentile, indicating poor analogies between the modern and fossil datasets. An explanation for this is the strong underrepresentation of larger stomatocyst types (>8 μm) in the sediment core in comparison to the sediment trap sample from the same lake. Fig. 6 shows possible nuisance factors that are discussed below, and Fig. 7 shows the reconstruction of 'Days$T_{4\,°C}$' since AD 1920, based on fossil stomatocyst assemblages analyzed in the sediment core from L. Escondida. The number of consecutive cold days varied between 110 and 160 days (note the inverted y-axis in Fig. 7) which is well within the range of Days$T_{4\,°C}$ in the training set. From AD 1930 to 1955, 'Days$T_{4\,°C}$' was generally low, indicating shorter cold seasons. Minimum values were reconstructed around AD 1954, where ice cover was only 110 days (in comparison to 136 days measured in AD 2011). After this minimum, values generally increased until ca AD 1980, with maximum values around AD 1967, 1983 and 1992. After AD 1980 the duration of the cold period displays a shortening trend towards the present day.

5. Discussion

5.1. Proxy interpretation and model performance

To develop a TF we used the proxy 'Days$T_{4\,°C}$', derived from the thermistor data. This proxy was used because the direct water temperature measurements were truncated. The number of consecutive days that surface waters are around 4 °C warm is an ecologically important proxy because it indicates the duration of the coldest period within the lake. For 16 out of 23 lakes, it also implied that the lake was ice covered during this time. For all lakes with ice cover, the ice covered period fell within the period June–November. As expected, 'Days$T_{4\,°C}$' was most strongly correlated with measured winter–spring (JJASON) surface water temperatures ($R = -0.98$, $p < 0.001$). Despite this high correlation with water temperatures, 'Days$T_{4\,°C}$' cannot be interpreted directly in terms of air temperature. The duration of ice cover is influenced by a number of other environmental factors such as wind and precipitation and the presence or absence of a snow cover on the ice (e.g. Livingstone, 1997; De Jong and Kamenik, 2011). Nevertheless, the analyses show that winter length forms an important control on modern stomatocyst assemblages in the study area. This is true for the lakes that were frozen in winter 2012, as well as for those that did not freeze over.

Pla-Rabés and Catalan (2011) explain the relation between stomatocyst composition and ice cover through the impact of winter–spring temperatures on spring mixing. They stress the importance of the characteristics (intensity and length) of this mixing phase and indicate that spring overturn is the key period determining nutrient availability all through the year (Pla-Rabés and Catalan, 2011). This in turn is a key factor in the species composition and development of phytoplankton and primary productivity (Reynolds 1989). A long period of ice cover would cause a short, intense phase of spring mixing that is terminated by the development of summer stratification. Consequently, nutrients may not be completely recycled and could remain available for the fall overturn (Pla-Rabés and Catalan, 2011). In lakes where ice cover is short or absent, spring mixing can take place earlier and over a longer time period (for monomictic lakes; overturn all through the

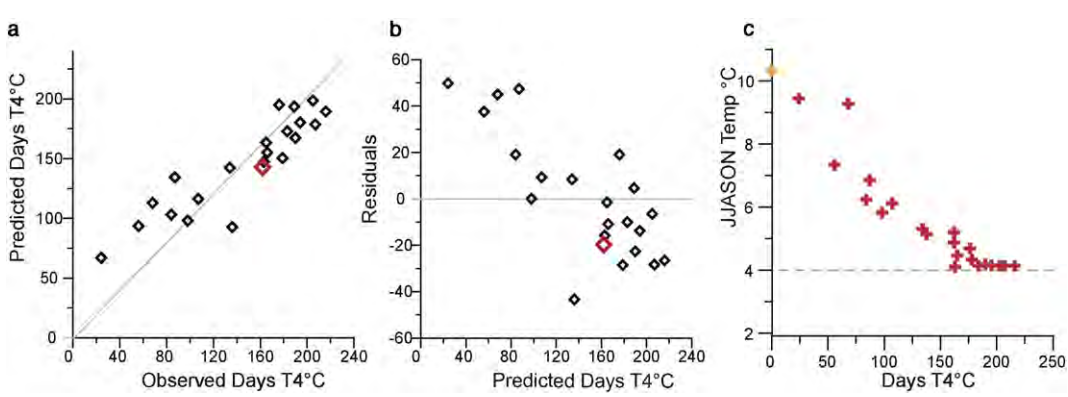

Fig. 3. Performance of the minimal adequate model WA-PLS2, which was based on 23 lakes spaced along a 1300 m altitude gradient, indicated by a) observed and predicted 'Days$T_{4\,°C}$' ($R_{boot} = 0.8$) and b) model residuals. Values for Laguna Escondida are shown as red diamonds in a) and b).The relation between measured 'Days$T_{4\,°C}$' and measured June–November surface water temperatures is shown in c). The truncation of surface water temperatures at 4 °C is clearly visible and was found in all lakes above 1100 m (see text).

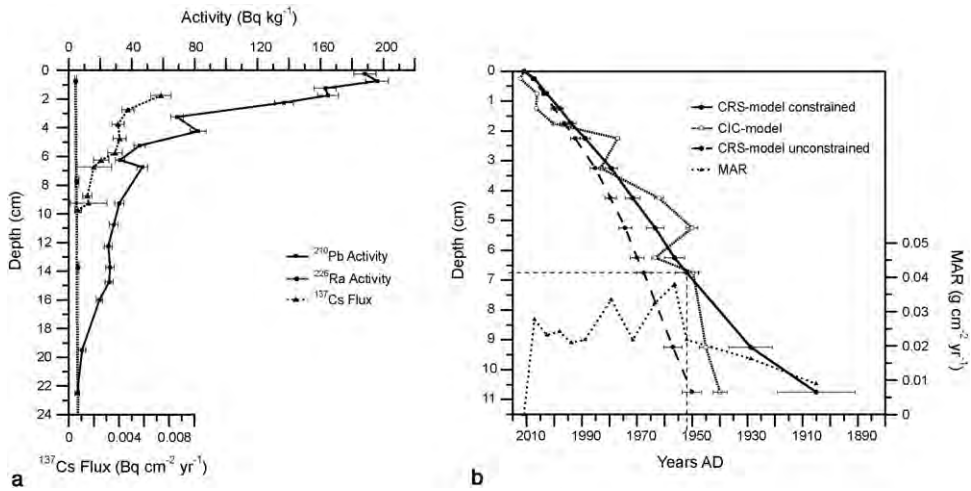

Fig. 4. a) Shows the measured activities of ^{210}Pb, ^{226}Ra and the ^{137}Cs flux values for the top 24 cm of sediment from Laguna Escondida. b) Age-depth models were based on the CIC model and the CRS model. For the CRS model, an unconstrained and a constrained version were calculated.

winter–spring season), thus prolonging the period during which nutrients are available and focusing this period on the spring–early summer season. This would clearly influence cyst composition through differences in seasonal succession and different combinations of water temperature and nutrient availability.

The finding that stomatocyst composition is closely related to winter–spring temperatures is in good agreement with findings from the Austrian (Kamenik and Schmidt, 2005) and Swiss Alpine (De Jong and Kamenik, 2011; De Jong et al., 2013) regions, as well as with studies in the Spanish Pyrenees (Pla and Catalan, 2005). Thus, the study demonstrates the reliability of stomatocysts as a proxy for cold-season climate variability, and confirms that the method can be applied successfully in a new geographical and geological setting. Since so far very few natural proxies are known that reflect the cold season, the stomatocyst-methodology may provide highly useful information for other regions as well.

A clear advantage of the stomatocyst training set was that it was developed using sediment traps and *in situ* measurements of surface water temperatures (following Kamenik and Schmidt, 2005). Because the sedimentation rates in high altitude lakes in our study are very low, this approach has major advantages over the commonly used method where surface sediment samples are used, often in combination with meteorological data extrapolated from the nearest station. In the current TF, stomatocysts accumulated in the traps over one year were linked directly to surface water temperatures. Using this approach, uncertainties concerning the number of years covered by a surface sample or the representativeness of meteorological data for a given lake were avoided. This approach may partly explain the very good performance statistics (high R^2 and small RMSEP in relation to the SD) of the WA-PLS2 model. A disadvantage of the current training set is that it was based on a small number of 23 lakes. Small training sets may be influenced strongly by outliers, however, as shown in Fig. 3, this is not the case in our model once Lake Menetue was removed. The trend in the residual structure of the WA-PLS model may point to an influence of variables other than 'DaysT$_{4\ °C}$'. However, according to Birks (1998) the trend in the residuals is also characteristic to PLS and WA-PLS models, and in addition, small datasets like the current one are more sensitive to this problem.

Although Transfer Function model performance is excellent for 'DaysT$_{4\ °C}$', the explorative statistics indicate that caution is needed in the interpretation of a reconstruction based on this model, in particular with reference to the identified possible nuisance variables. In addition to 'DaysT$_{4\ °C}$', two other variables were shown to influence the dataset: Si and Conductivity. In Fig. 6 we explored the characteristics of the most important measured 'confounding variables'; variables that co-vary with 'DaysT$_{4\ °C}$' along the altitude (and hence stomatocyst) gradient and therefore potentially enhance model performance statistics (Juggins, 2013). The $\lambda 1/\lambda 2$ value for 'DaysT$_{4\ °C}$' was 0.8, which also indicates that there is another(or composite) variable which better explains the variability in the stomatocyst dataset (Juggins, 2013).

Fig. 6 shows 'DaysT$_{4\ °C}$', Si and Conductivity along lake elevation. Dissolved silica (Fig. 6b) is only weakly correlated with altitude but

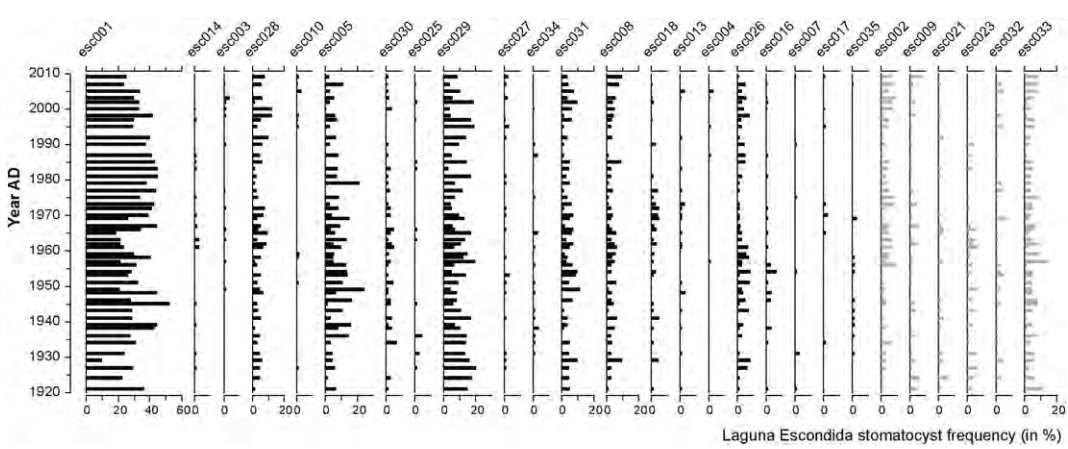

Fig. 5. Stomatocyst stratigraphy for L. Escondida, showing stomatocyst assemblage changes since AD 1920. Only stomatocysts that exceeded 2% and occurred in >2 samples are shown. Stomatocyst types were ordered along their response to 'DaysT$_{4\ °C}$' in a partial CCA. Types shown to the right (in gray) were not included in the TF.

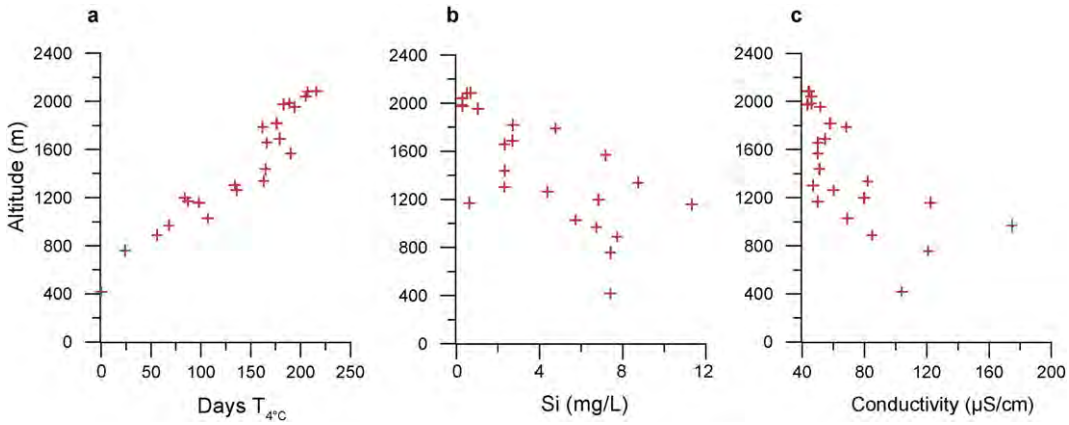

Fig. 6. This figure shows the most important environmental variables that influenced stomatocyst assemblages in the training set lakes, plotted along altitude: a) $DaysT_{4\,°C}$, b) Si content and c) lake water conductivity.

declines with higher altitudes. The correlation for conductivity with altitude is also weak, mostly because all but six lakes show very low conductivity values of ≤80 μS/cm. It therefore seems likely that although the overall gradient of conductivity follows the altitude gradient, conductivity primarily influences stomatocyst composition in the low altitude lakes where conductivity is highest. A possible cause for the co-variance of Si and Conductivity along altitude is the influence of chemical weathering and hence the presence and thickness of soils. The uppermost lakes were situated in sparsely vegetated catchments with patchy, thin soils and a predominance of scree slopes and bedrock outcrops. Combined with the low temperatures and long period of snow cover in the catchment at high altitudes, chemical weathering is minimal and soil formation and vegetation development are correspondingly low. This setting likely explains the exceptionally low values for lake water nutrients, ions and conductivity values at high altitudes. At lower altitudes, with high summer temperatures, thick soils and dense vegetation create a strong altitudinal contrast. Over long time scales, these contrasts are clearly also primarily temperature driven. Because no reliable data on the amount and type of precipitation was available, this factor could not be explored further. However, at longer time scales, driven by the position of the Westerlies, high precipitation and mild winters are expected to co-vary. At shorter timescales, land use changes likely influenced the lower altitude lakes to some extent.

A number of other studies have found that conductivity can be an important control on stomatocyst assemblages (e.g. Pla and Anderson, 2005; Hernández-Almeida et al., 2014). Thus, as expected for all training sets that are designed along a strong geographical gradient, variables other than the one of interest co-vary along the chosen gradient. Caution is therefore needed when making reconstructions back in time based on this Transfer Function. In particular, natural as well as human induced changes in Conductivity or Si content over time should be considered when interpreting a reconstruction of '$DaysT_{4\,°C}$' back in time. If such disturbances are likely to have taken place, or better, if these can be demonstrated with additional analyses, the reconstructed temperatures during such phases are unreliable.

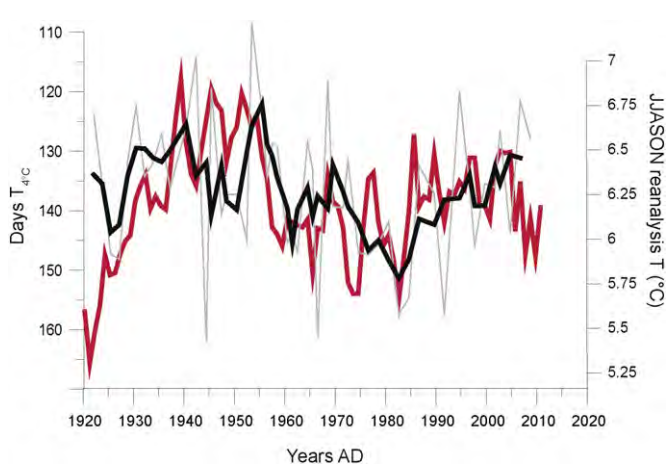

Fig. 7. Reconstructed variability in '$DaysT_{4\,°C}$' showing 5-year filtered data (black line) and unfiltered data (gray line). Note the inverted y-axis; a lower number of '$DaysT_{4\,°C}$' represents a shorter, hence relatively warmer winter–spring season. The red line represents reanalysis temperature data for the grid cell (0.5° × 0.5°) encompassing Laguna Escondida.

5.2. Reconstructed '$DaysT_{4\,°C}$' from AD 1920 to present

To assess whether the TF model was able to capture past temperature variability in a down core analysis, the TF was applied to the sediments of L. Escondida. This lake was selected because it is a highly remote lake with minimal human influence in its small, simple catchment. Statistically, it sits in the mid-range of the model and therefore past variability in $DaysT_{4\,°C}$ was expected to fall within the range of the modern training set lakes. In addition, modern conductivity and Si values are low (68 μS cm^{-1}, 4.7 mg l^{-1}), indicating low ion inflow despite relatively high rainfall. Therefore we expect that the variability of conductivity and Si content back in time (until AD 1920) must be minimal, and that the reconstruction shown in Fig. 7 primarily reflects changes in winter length.

In Fig. 7, reconstructed '$DaysT_{4\,°C}$' back to AD 1920 were compared to reanalysis data (0.5° × 0.5° grid cell encompassing the study site; Mitchell and Jones, 2005) for the months JJASON. The comparison shows overall highly similar multi-decadal and decadal trends. The high similarity between these independent datasets forms a clear indication that the stomatocyst–'$DaysT_{4\,°C}$' TF can be used to reliably reconstruct past climatic variability in L. Escondida, at least back until AD 1920. The total amplitude of '$DaysT_{4\,°C}$' indeed falls within the range of the TF, so that no extrapolation was required for the reconstruction.

Reconstructed winter severity displays a clear warming trend since AD 1980. In L. Escondida, the duration of ice cover on the lake in AD 1983 (±5 years) lasted for more than 150 days, whereas in recent time, the ice cover period was ca. 25 days shorter. Although this warming trend is substantial, the reconstruction also shows that recent warming (until AD 2009) is not exceptional in the context of the past century. For example, the periods around AD 1940 and from AD 1950–1955 (Fig. 7) were warmer. This is also shown in the reanalysis data for this region (Fig. 7) and was also observed by Neukom et al. (2010b) and Neukom and Gergis (2011) for Patagonia and central Chile. Similarly, based on tree ring analyses from the upper tree limit in northern Patagonia, Villalba et al. (2003) found that the period just before AD 1950 was substantially warmer than more recent decades.

Warming in the Andes of southern South America since AD 1980 is thus substantial, but does not currently exceed measured or reconstructed warm temperatures during the past 100 years. This is true for the summer season as well as for the winter–spring season as demonstrated here.

The warming that started in AD 1980 in the reconstruction from Laguna Escondida continues up until the present time. Interestingly, this trend is in direct contrast to several coastal meteorological station data in Chile from 17 to 37°S (Falvey and Garreaud, 2009). Coastal stations and ocean observation data in this region show a cooling trend of −0.2 °C from AD 1978 to 2006, whereas these authors also found a simultaneous warming in the Andes. This high altitude warming is now also confirmed by our study, which is highly relevant because meteorological stations at high elevations are absent in this region. This implies that the coast-high elevation temperature contrast is confirmed independently and just south of the region indicated by Falvey and Garreaud (2009). This location is at the edge of the main activity band of the Southern Hemisphere Westerlies in winter (Garreaud et al., 2009). The cause for the observed contrast was, according to Falvey and Garreaud (2009), the intensified South Pacific Anticyclone (SPAC). In their model runs, a more intense SPAC was also a consequence of global warming. A southward contraction of the Westerlies, which is in agreement with a more intense SPAC, was also described by Cai (2006) from observational data, and by Yin (2005) and Sen Gupta et al. (2009) in model projections.

Our study illustrates that the effects of a more intense SPAC also cause high-altitude warming down to 38°S and possibly further. This is a region that is commonly associated with strong westerlies and hence minimal temperature contrasts between high and low altitudes. The Westerlies are also the cause of high winter precipitation rates, in particular along the western flanks of the Andes (Lamy et al., 2010). A strengthening of the SPAC and corresponding southward shift of northern margin of the Westerlies wind belt would thus influence high altitude regions in two ways: winter warming (Falvey and Garreaud, 2009; this study) and reduced precipitation (e.g. Mayewski et al., 2015). In a country that largely depends on snow melt from the Andes for its water supply these changes could potentially have severe implications.

6. Conclusions

The results of this study support Juggins (2013) suggestions that training set data should be explored carefully and the effect of confounding variables should be addressed adequately. However, the study also provides important support for the Transfer Function concept. The reconstruction compares very well to independent temperature data since AD 1920. This finding is highly important because it illustrates that, despite the non-ideal performance statistics for 'Days$T_{4\ °C}$' as an explanatory variable, the TF yields results that are consistent with measurement data. We therefore propose to combine the statistical analyses and suggestion by Juggins (2013) with detailed, high resolution down core analyses for the calibration period. This allows for an independent assessment of the reliability of the TF model. This study illustrates that although 'Days$T_{4\ °C}$' is not an ideal proxy in terms of its λ1/λ2 value, and the TF model likely has 'boosted' performance statistics, reliable environmental reconstructions can be made using the stomatocyst–'Days$T_{4\ °C}$' Transfer Function. In our opinion the quantitative approach using Transfer Functions is not 'sick science' (Juggins, 2013). However, quantitative reconstructions do require thorough data analysis, discussion and analysis of possible confounding variables, a comparison to fully independent (meteorological) records and careful site and proxy selection. In particular, past variability in known co-varying variables that were identified for a specific training set should be considered prior to site selection for reconstructions. Ideally, a multi-proxy approach is applied so that the influence of these confounding variables can be reconstructed independently. If confounding variables are found to vary strongly through time, any reconstruction based on the used training set is unreliable. However, if confounding variables can be expected or demonstrated to have been relatively stable, the Transfer Function likely yields reliable results.

The reconstruction of 'Days$T_{4\ °C}$' from L. Escondida compares very well with reanalysis data. This is an independent confirmation of the reliability of the TF model, at least when applied to L. Escondida and for the time period under consideration in this study. This finding also indicates that the relatively novel, quantitative stomatocyst methodology can be applied successfully in mountain areas such as the Chilean Andes. Because stomatocysts reflect cold season climatic conditions, this methodology may provide highly useful data in other future studies as well.

The reconstruction of winter severity shows a clear warming trend since AD 1980. In the context of the past century, however, the current warmth is not exceptional. This is in agreement with other findings from Southern South America; however, it is in strong contrast to most temperature reconstructions made for the Northern Hemisphere. In addition, the warming continues up to the most recent year in the reconstruction. This is in agreement with other records from high altitudes north of 38°S and confirms the contrast between high and low altitude temperature patterns that was described by Falvey and Garreaud (2009). Moreover, it expands the range of altitudinally contrasting temperature trends, and hence the influence range of the South Pacific Anticyclone, down to 38°S. This is a region that, in winter, is associated with the Southern Hemisphere Westerlies. This study clearly shows that low altitude temperature measurements do not necessarily reflect high altitude temperature patterns. In such cases, when meteorological stations are absent at high altitudes, high-quality climatic reconstructions are required to reconstruct even recent climatic changes.

Supplementary data to this article can be found online at http://dx.doi.org/10.1016/j.gloplacha.2015.12.006.

Acknowledgments

We greatly appreciate the comments and suggestions of two anonymous reviewers. We want to thank S. Hagnauer and D. Fischer for laboratory assistance and help with fieldwork preparations. Fieldwork was made possible with the help of M. Engelsman, K. Saunders, S. Hunziker, P. Jana Pinninghoff, M. Gatica Rivera, J. van Wichelen, R. Urrutia and A. Araneda. Permissions to carry out fieldwork in National Parks and in the border region of Chile were kindly granted by the Chilean CONAF (Corporación Nacional Forestal) and the Chilean DIFROL (Dirección Nacional de Fronteras y Límites del Estado). This study was funded by a Swiss National Science Foundation (Ambizione) grant (PZ00P2_131797/1) and an EU-ERG grant (PERG08-GA-2010-276703) to R. de Jong.

References

Appleby, P.G., 2001. Chronostratigraphic techniques in recent sediments. In: Last, W.M., Smol, J.P. (Eds.), Tracking Environmental Change Using Lake SedimentsBasin Analysis, Coring and Chronological Techniques vol. 1. Kluwer Academic Publishers, Dordrecht, The Netherlands, pp. 171–201.

Basran, M., 2011. Handbook of Environmental Isotope Geochemistry. vol. I, Springer, Berlin (951 pp. ISBN978-3-642-10636-1).

Birks, H.J.B., 1995. Quantitative palaeoenvironmental reconstructions. In: Maddy, D., Brew, J.S. (Eds.), Statistical Modeling of Quaternary Science Data. Quaternary Research Association, Cambridge, p. 271.

Birks, H.J.B., 1998. Numerical tools in palaeolimnology—progress, potentialities, and problems. J. Paleolimnol. 20, 307–332.

Blanchet, F.G., Legendre, P., Borcard, D., 2008. Forward selection of explanatory variables. Ecology 89, 2623–2632.

Bloesch, J., Burns, N., 1980. A critical review of sedimentation trap technique. Schweiz. Z. Hydrol. 42, 15–55.

Cai, W., 2006. Antarctic ozone depletion causes an intensification of the Southern Ocean super-gyre circulation. Geophys. Res. Lett. 33, L03712.

De Jong, R., Kamenik, C., 2011. Validation of a chrysophyte stomatocyst-based cold-season climate reconstruction from high-Alpine Lake Silvaplana, Switzerland. J. Quat. Sci. 26, 268–275. http://dx.doi.org/10.1002/jqs.1451.

De Jong, R., Kamenik, C., Westover, K., Grosjean, M., 2013. A chrysophyte stomatocyst-based reconstruction of cold-season air temperature from Alpine Lake Silvaplana (AD 1500–2003); methods and concepts for quantitative inferences. J. Paleolimnol. 50, 519–533. http://dx.doi.org/10.1007/s10933-013-9743-5.

Dray, S., Legendre, P., Blanchet, G., 2013. packfor: Forward Selection with permutation URL http://r-forge.r-project.org/projects/sedar/.

Duff, K.E., Zeeb, B.A., Smol, J.P., 1995. Atlas of Chrysophycean Cysts. vol. 1. Kluwer Academic Publishers, Dordrecht.

Falvey, M., Garreaud, R.D., 2009. Regional cooling in a warming world: recent temperature trends in the southeast Pacific and along the West Coast of subtropical South America (1979–2006). J. Geophys. Res. 114, D04102. http://dx.doi.org/10.1029/2008JD010519.

Garreaud, R.D., Vuille, M., Compagnucci, R., Marengo, J., 2009. Present-day South American climate. Palaeogeogr. Palaeoclimatol. Palaeoecol. 281, 180–195. http://dx.doi.org/10.1016/j.palaeo.2007.10.032.

Garreaud, R., Lopez, P., Minvielle, M., Rojas, M., 2013. Large-scale control on the Patagonian climate. J. Clim. 26, 215–230. http://dx.doi.org/10.1175/JCLI-D-12-00001.1.

Grasshoff, K., 1976. Determination of nitrate and nitrite. In: Grasshoff, K. (Ed.), Methods of Seawater Analysis. Verlag Chemie, Weinheim, New York, p. 317.

Hernández-Almeida, I., Grosjean, M., Tylmann, W., Bonk, A., 2014. Chrysophyte cyst-inferred variability of warm season lake water chemistry and climate in northern Poland: training set and downcore reconstruction. J. Paleolimnol. http://dx.doi.org/10.1007/s10933-014-9812-4.

Jones, P.D., Briffa, K.R., Osborn, T.J., et al., 2009. High-resolution palaeoclimatology of the last millennium: a review of current status and future prospects. The Holocene 19, 3–49.

Juggins, S., 2003. C2 user guide. Software for Ecological and Palaeoecological Data Analysis and Visualisation.

Juggins, S., 2013. Quantitative reconstructions in palaeolimnology: new paradigm or sick science? Quat. Sci. Rev. 64, 20–32. http://dx.doi.org/10.1016/j.quascirev.2012.12.014.

Kamenik, C., Schmidt, R., 2005. Chrysophyte resting stages: a tool for reconstructing winter/spring climate from Alpine lake sediments. Boreas 34, 477–489. http://dx.doi.org/10.1080/03009480500231468.

Koroleff, F., 1976. Determination of ammonia, phosphorus and silicon. In: Grasshoff, K. (Ed.), Methods of Seawater Analysis. Verlag Chemie, Weinheim, New York, p. 317.

Lamy, F., Kilian, R., Arz, H.W., et al., 2010. Holocene changes in the position and intensity of the southern westerly wind belt. Nat. Geosci. 3, 695–699.

Livingstone, D.M., 1997. Break-up dates of Alpine lakes as proxy data for local and regional mean surface air temperature. Clim. Chang. 37, 407–439.

Mayewski, P.A., Bracegirdle, T., Goodwin, I., Schneider, D., Bertler, N.A.N., Birkel, S., Carleton, A., England, M.H., Kang, J.-H., Khan, A., Russell, J., Turner, J., Velicogna, I., 2015. Potential for Southern Hemisphere climate surprises. J. Quat. Sci. 30, 391–395.

Mitchell, T.D., Jones, P.D., 2005. An improved method of constructing a database of monthly climate observations and associated high-resolution grids. Int. J. Climatol. 25, 693–712.

Neukom, R., Gergis, J., 2011. Southern Hemisphere high-resolution palaeoclimate records of the last 2000 years. The Holocene 22, 501–524. http://dx.doi.org/10.1177/0959683611427335.

Neukom, R., Luterbacher, J., Villalba, R., Küttel, M., Frank, D., Jones, P.D., Grosjean, M., Esper, J., Lopez, L., Wanner, H., 2010a. Multi-centennial summer and winter precipitation variability in southern South America. Geophys. Res. Lett. 37, 1–23. http://dx.doi.org/10.1029/2010GL043680.

Neukom, R., Luterbacher, J., Villalba, R., Küttel, M., Frank, D., Jones, P.D., Grosjean, M., Wanner, H., Aravena, J.-C., Black, D.E., Christie, D.a., D'Arrigo, R., Lara, a., Morales, M., Soliz-Gamboa, C., Srur, a., Urrutia, R., Gunten, L., 2010b. Multiproxy summer and winter surface air temperature field reconstructions for southern South America covering the past centuries. Clim. Dyn. 37, 35–51. http://dx.doi.org/10.1007/s00382-010-0793-3.

Oksanen, J., Guillaume, B.F., Kindt, R., Legendre, P., Minchin, P.R., O'Hara, R.B., Simpson, G.L., Solymoy, P., Henry, M., Stevens, H., Wagner, H., 2013. vegan: Community ecology package URL http://cran.r-project.org/package=vegan.

PAGES 2 k Consortium, 2013. Continental-scale temperature variability during the last two millennia. Nat. Geosci. 6 (339–346), 2013. http://dx.doi.org/10.1038/NGEO1797.

Parada, M.A., Lopez-Escobar, L., Oliveros, V., Fuentes, F., Morata, D., Calderón, M., Aguirre, L., Féraud, G., Espinoza, F., Moreno, H., Figueroa, O., Muñoz Bravo, J., Vasquez, T., C. R., S., 2007. Andean magatism. In: Moreno, T., Gibbons, W. (Eds.), The Geology of Chile. The Geological Society, London, pp. 115–146.

Pla, S., Anderson, N.J., 2005. Environmental factors correlated with chrysophyte cyst assemblages in low Arctic lakes of southwest Greenland. J. Phycol. 41, 957–974. http://dx.doi.org/10.1111/j.1529-8817.2005.00131.x.

Pla, S., Catalan, J., 2005. Chrysophyte cysts from lake sediments reveal the submillennial winter/spring climate variability in the northwestern Mediterranean region throughout the Holocene. Clim. Dyn. 24, 263–278. http://dx.doi.org/10.1007/s00382-004-0482-1.

Pla, S., Camarero, L., Catalan, J., 2003. Chrysophyte cyst relationships to water chemistry in Pyrenean lakes (NE Spain) and their potential for environmental reconstruction. J. Paleolimnol. 30, 21–34.

Pla-Rabés, S., Catalan, J., 2011. Deciphering chrysophyte responses to climate seasonality. J. Paleolimnol. 46, 139–150.

Reynolds, C.S., 1989. Physical determinants of phytoplankton succession, p. 9–56. In: Sommer, U. (Ed.), Plankton ecology, succession in plankton communities. Springer, Berlin Heidelberg, p. 364. http://dx.doi.org/10.1007/978-3-642-74890-5_2.

Sen Gupta, A., Santoso, A., Taschetto, A.S., Ummenhofer, C.C., Trevena, J., England, M.H., 2009. Projected changes to the Southern Hemisphere ocean and sea ice in the IPCC AR4 climate models. J. Clim. 22, 3047–3078.

Servicio Nacional de Geologia y Mineria, 2003. Mapa Geologico de Chile: Version Digital, Escala 1:1,000,000 4.

Telford, R.J., Birks, H.J.B., 2011. A novel method for assessing the statistical significance of quantitative reconstructions inferred from biotic assemblages. Quat. Sci. Rev. 30, 1272–1278. http://dx.doi.org/10.1016/j.quascirev.2011.03.002.

Ter Braak, C.J.F., 1987. The analysis of vegetation–environment relationships by canonical correspondence analysis. Vegetatio 69, 69–77.

Ter Braak, C.J.F., 1988. Canoco—A FORTRAN Program for Canonical Community Ordination by (Partial) (Detrended) (Canonical) Correspondence Analysis, Principal Components Analysis and Redundancy Analysis. GLW, Wageningen.

Trachsel, M., Grosjean, M., Schnyder, D., Kamenik, C., Rein, B., 2010. Scanning reflectance spectroscopy (380–730 nm): a novel method for quantitative high-resolution climate reconstructions from minerogenic lake sediments. J. Paleolimnol. 44, 979–994. http://dx.doi.org/10.1007/s10933-010-9468-7.

Villalba, R., Lara, A., Boninsegna, J.A., Masiokas, M., Delgado, S., Aravena, J.C., Roig, F.A., Schmelter, A., Wolodarsky, A., Ripalta, A., 2003. Large-scale temperature changes across the southern Andes: 20th-century variations in the context of the past 400 years. Clim. Chang. 177–232.

Von Gunten, L., Grosjean, M., Beer, J., Grob, P., Morales, A., Urrutia, R., 2009. Age modeling of young non-varved lake sediments: methods and limits. Examples from two lakes in Central Chile. J. Paleolimnol. 42, 401–412. http://dx.doi.org/10.1007/s10933-008-9284-5.

Walsh, C., Mac Nally, R., 2013. hier.part: hierarchical partitioning URL http://cran.r-project.org/package=hier.part.

Wilkinson, A.N., Zeeb, B.A., Smol, J.P., 2001. Atlas of Chrysophycean Cysts. 2. Kluwer Academic Publishers, Dordrecht.

Yin, J.H., 2005. A consistent poleward shift of the storm tracks in simulations of 21st century climate. Geophys. Res. Lett. 32, L18701. http://dx.doi.org/10.1029/2005GL023684.

Zeeb, B., Smol, J., 1995. A weighted-averaging regression and calibration model for inferring lakewater salinity using chrysophycean stomatocysts from lakes in western Canada. Int. J. Salt Lake Res. 4, 1–23.